Journal of Physics: Conference Series

Modeling of supersonic gas flows in radial nozzles

To cite this article: S P Kiselev *et al* 2019 *J. Phys.: Conf. Ser.* **1268** 012033

Modeling of supersonic gas flows in radial nozzles

S P Kiselev[1,2], V P Kiselev[1] and V N Zaikovskii[1]

[1]Khristianovich Institute of Theoretical and Applied Mechanics, Russian Academy of Sciences, Siberian Branch, 630090 Novosibirsk, Russia
[2]Novosibirsk State Technical University, 630092 Novosibirsk, Russia

E-mails: kiselev@itam.nsc.ru, kiselevvp@itam.nsc.ru, zaikovskii@itam.nsc.ru

Abstract. In the present paper, we report on the results of a study of supersonic gas flows in a radial nozzle. The pressurized gas is supplied into a circular channel, from which it then flows into the gap between two parallel disks (radial nozzle). It is shown that the structure of the jet ejected into ambient space substantially depends on the friction force acting on the gas flow from the side of the disks. The force of friction leads to a considerable decrease of the velocity of the supersonic jet, which acquires a fan-shaped form instead of being barrel-shaped. The numerical results proved to be in good agreement with experimental data.

1. Introduction

Until recently, little attention was paid by researchers to supersonic flows in radial nozzles. In [1], gas flows in wider nozzles at lower pre-chamber pressures as compared with the present study were investigated. In papers [2], flow pulsations in radial supersonic jets arising in radial nozzles with a width also much greater in comparison with the nozzle investigated in the present work were examined. However, the situation has now changed as new technologies using radial nozzles have emerged. In publication [3], it was shown that radial nozzles can be used in cold gas-dynamic spraying to apply coatings onto the inner surfaces of pipes. The essence of this method is acceleration of microparticles in a supersonic jet impinging onto an obstacle. A coating is formed on the obstacle as a result of collision of accelerated microparticles. In [4, 5], the structure of pseudo-shocks in radial micro-nozzles was studied. In the present article, we report on the results of a study of supersonic jets ejected from a circular channel into the slot of a radial nozzle.

2. Experimental procedure

Diagram of a radial nozzle is shown in figure 1, where the nozzle cross-sections in the planes (x, y) and (x, z) (figures 1 (a) and 1 (b), respectively) are shown. The radial nozzle consists of two disks of radius $r_e = 36$ mm, both fitted onto a central rod of radius r_0 (the rod is shown in figures 1 (a) in black colour). The spacing between the disks h was varied by displacing the external disk along the rod. Into the space between the disks, an circular gasket with internal radius $r_0 = 5$ mm, external radius $r_2 = 20$ mm, and width h equal to the gap between the disks was inserted. In the gasket, a cut of length a and width b was made along the axis x. As a result, a planar channel of length a, height b, and width h was formed at the inlet to the radial nozzle (this channel is shown in figure 1 (a) with dashed lines). The channel began in the section $x = x_i$ and ended in the section $x = r_2$. The gas under pressure p_0 was fed into the channel from a pre-chamber, which was a cylindrical tube with internal radius $r_0 = 5$ mm and external radius $r_1 = 9$ mm (see figure 1 (b)). Then, the gas flowed from the channel to the radial nozzle; the streamlines of the flow are conventionally shown in figure 1 with arrowed lines.

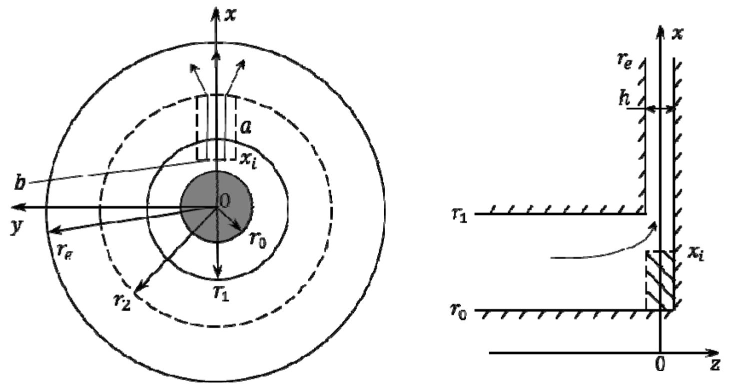

(a) (b)

Figure 1. Gas flow in the radial nozzle.

As the working gas, cold air with temperature $T_0 = 300$ K was used. In different experiments, the gas pressure p_0 in the pre-chamber varied in the range $0.9 \text{ MPa} \le p_0 \le 1.0 \text{ MPa}$. The gas from the radial nozzle was ejected into ambient space, which was filled with air under normal conditions (pressure $p_\infty = 0.1$ MPa, temperature $T_\infty = 300$ K). In the experiments, the pressure on the surface of the external disk was measured using 11 pressure taps of diameter $d_i = 0.8$ mm made on this surface and arranged in radial direction. The pressure taps were connected with pneumometric tubes to KIM strain-gauge pressure sensors (developed at ITAM SB RAS). The accuracy of the static-pressure measurements was 0.5%.

3. Numerical simulation

In publications [4, 5], it was shown that the channel approximation can be used in calculating the supersonic gas flows in a radial nozzle of width $h < 2$ mm, in which all gas parameters do not depend on the transverse coordinate, and the influence due to the nozzle walls was taken into account by adding the friction force to the right-hand side of the gas motion equation. The equations of the two-dimensional model result from the averaging of the three-dimensional equations over the cross section. The equations of continuity, motion and gas energy for average flow quantities are:

$$\frac{\partial A}{\partial t} + \frac{\partial F}{\partial x} + \frac{\partial G}{\partial y} + H = 0, \quad p = \rho RT, \quad e = C_v T, \quad \mu = \mu_0 \left(\frac{T_0 - T_1}{T - T_1}\right)\left(\frac{T}{T_0}\right)^{3/2}, \quad \mathbf{v}^2 = u^2 + v^2,$$

$$A = \begin{pmatrix} \rho \\ \rho u \\ \rho v \\ \rho\left(e + \mathbf{v}^2/2\right) \end{pmatrix}, \quad F = \begin{pmatrix} \rho u \\ \rho u^2 + p \\ \rho uv \\ \rho u\left(e + p/\rho + \mathbf{v}^2/2\right) \end{pmatrix}, \quad G = \begin{pmatrix} \rho v \\ \rho vu \\ \rho v^2 + p \\ \rho v\left(e + p/\rho + \mathbf{v}^2/2\right) \end{pmatrix}, \quad H = \begin{pmatrix} 0 \\ \tau_x \\ \tau_y \\ 0 \end{pmatrix}, \quad (1)$$

$$\tau_x = C_f \rho u |\mathbf{v}| / h, \quad \tau_y = C_f \rho v |\mathbf{v}| / h, \quad C_f = 12/Re + 0{,}06/\left(2Re\right)^{0{,}25}, \quad \mathrm{Re} = \rho |\mathbf{v}| h / \mu.$$

where ρ, p, e and T are the gas density, the gas pressure, the specific internal energy, and the gas temperature; u and v are the velocity components along the x- and y- axes; $\mathbf{v}^2$ is the squared velocity modulus; τ_x and τ_y are the components of the friction force acting on the gas flow from the side of the disks along the x- and y-axes; C_f, μ and C_v are the drag coefficient, the dynamic viscosity, and the thermal conductivity; and γ is the Poisson's adiabatic index. The Reynolds number Re in (1) was calculated at the temperature equal to the half-sum of the static gas temperature and the nozzle wall temperature $T' = (T + T_W)/2$. In the present work, the static temperature T was determined from the solution of system (1), and the wall temperature was taken equal to the flow stagnation temperature $T_W = T_0$. The effect due to viscosity leads to the appearance, in the right-hand sides of the equations of motion, of the friction force τ_x, τ_y acting on the gas from the side of the nozzle walls. The drag coefficient C_f involves two terms, of which the first gives the dependence for the laminar flow, and the second, for the turbulent flow. The influence due to the friction force on the main gas flow arises when the boundary layers developing on the opposite walls of the nozzle join together. With this in mind, in equations (1) it was assumed that $C_f = 0$ for $x - x_i < x_*$ and $C_f \neq 0$ for $x - x_i > x_*$. In the study of [4], it was shown that for close values of flow quantities the merging of the boundary layers occurs at a distance $x_* \approx 5$ mm from the nozzle inlet.

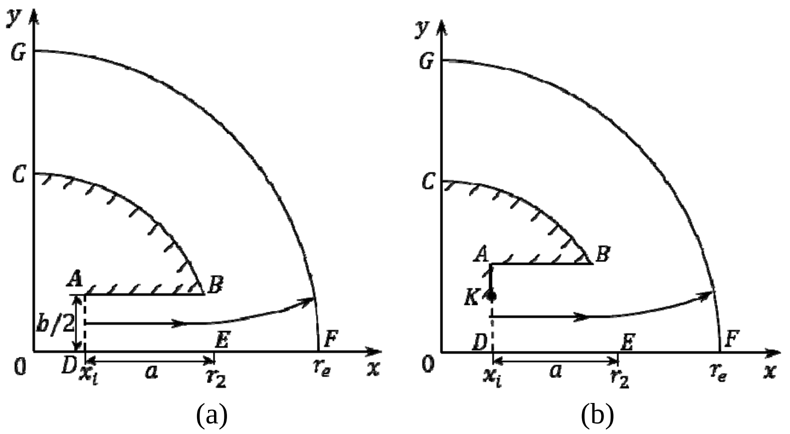

Figure 2. Computational domain: (a) – narrow channel; (b) – wide channel.

Numerical modelling of the gas flow was carried out in two-dimensional approximation (1), in the channel $x_i < x < r_2$, $0 < y < b/2$ and in the radial nozzle $r_2 < r < r_e$ (figure 2). In the present study, we analyzed the gas flows ejected from a narrow and wide channel (figures 2 (a) and (b), respectively) into the slot between the disks (radial nozzle). The gas entered the channel through the section AD (in the case of the narrow channel) and through the section KD (in the case of the wide channel). In both cases, the gas was ejected into the radial nozzle through the section BE. The arrowed lines in figure 2 show the streamlines of the flow. The solution of system (1) was sought for the following boundary conditions. By symmetry of the problem, a symmetry condition was adopted at the boundaries DF and CG (figure 2), and the slip condition was set on the shaded boundaries ABC and $KABC$. At the inlet to the channels, AD and KD, the pressure $p_i = 0{,}9\,p_0$ was specified for the incoming gas flow, and the velocity and temperature were determined similarly to [4, 5], using the isentropic formulas. At the exit from the nozzle, at the line GF, a boundary condition for gas ejection into the region with a gas under normal conditions, $p = p_\infty$ and $T = T_\infty$, was set. If the Mach number at the boundary was greater than unity ($\mathrm{M} > 1$), then the symmetry conditions were set at the boundary; otherwise ($\mathrm{M} < 1$) the boundary conditions were found from the relations on the characteristics [4, 5]. System (1) was solved numerically using the explicit Lax – Wendroff difference scheme [6]. In calculations according to this scheme, which involved flows with shock waves, the shock wave underwent smearing due to the scheme viscosity. The problem was solved by the relaxation method on a curvilinear difference grid. At the initial moment, the problem of discontinuity decay in the section

$x = x_0$, $x_i < x_0 < r_2$ was solved. On the left of the discontinuity, $x < x_0$, parameters like those in a high-pressure chamber, p_0, T_0, $u_0 = 0$ and $v_0 = 0$, were set, and on the right of the discontinuity, conditions like those at a nozzle outlet, $p_\infty, T_\infty, u_\infty = 0$ and $v_\infty = 0$, were specified. As a result of the discontinuity decay, there formed an established flow independent of time.

4. Discussion of calculated and experimental data

Figures 3 and 4 show the results of numerical calculations and experiments performed for the supersonic jets ejected into a slot of width $h = 0.2$ mm. The gas parameters in the pre-chamber were $p_0 = 1.0$ MPa and $T_0 = 300$ K. Figure 3 shows results of the study of a thin jet with $b = 4$ mm. Figure 3 (a) shows the distribution of Mach numbers $\mathrm{M}(x, y)$ calculated with taking into account the friction force, and figure 3 (b), the distribution of Mach numbers $\mathrm{M}(x, y)$ calculated without taking into account this force (in the latter case it was assumed that $C_f = 0$ in equations (1)). Figure 3 (c) shows the dependences of normalized pressure $p(x)/p_0$ on the coordinate x along the jet axis obtained experimentally and in numerical calculations. In the case of a thick jet with $b = 17$ mm, the flow was discharged from the hole KD of width $b' = 11$ mm.

The distributions of Mach numbers $\mathrm{M}(x, y)$ and the dependence of pressure on the coordinate along the jet axis $p(x)$ for a thick jet with $b = 17$ mm are shown in figure 4.

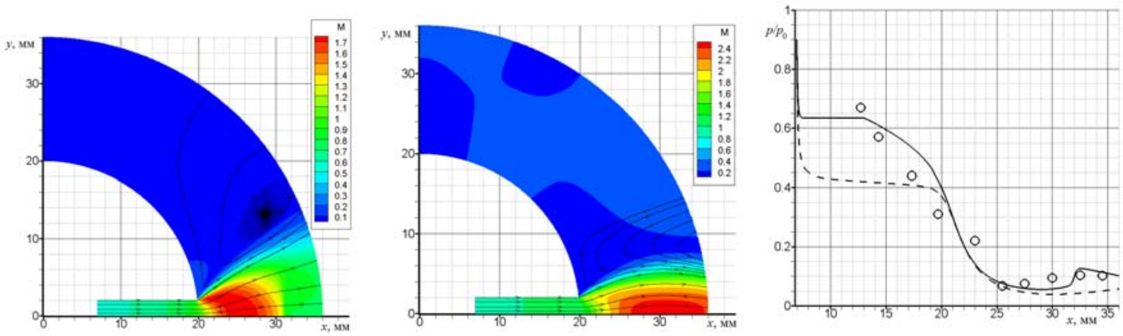

(a) (b) (c)

Figure 3. Calculated data for the steady-state flow at $a = 13$ mm and $b = 4$ mm : (a) – the distribution $\mathrm{M}(x, y)$ calculated with taking the friction force into account; (b) – the distribution $\mathrm{M}(x, y)$ calculated without taking the friction force into account ($C_f = 0$); (c) – the distribution $p(x, y)/p_0$ along the jet axis $y = 0$ (the circles are the experimental data, and the solid and dashed lines are the data calculated with and without taking the friction force into account).

IOP Conf. Series: Journal of Physics: Conf. Series **1268** (2019) 012033 doi:10.1088/1742-6596/1268/1/012033

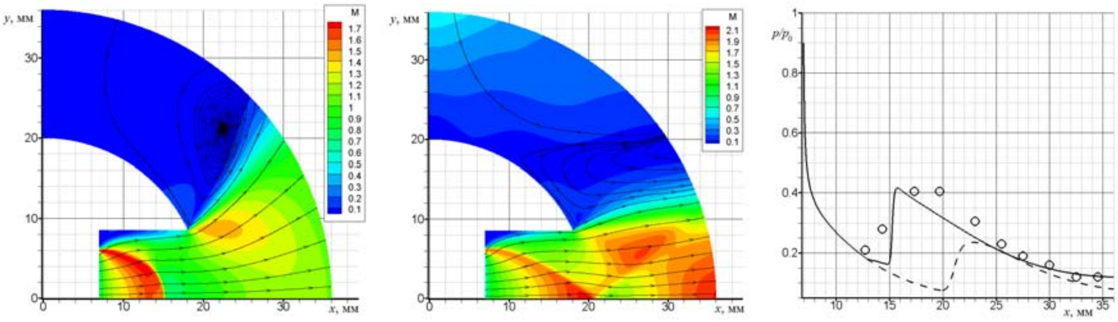

(a) (b) (c)

Figure 4. Calculated data for steady-state flow at $a = 13\,\mathrm{mm}$ and $b = 17\,\mathrm{mm}$, $b' = 11\,\mathrm{mm}$: (a) – the distribution $\mathrm{M}(x, y)$ calculated with taking the friction force into account; (b) – the distribution $\mathrm{M}(x, y)$ calculated without taking the friction force into account ($C_f = 0$); (c) – the distribution $p(x, y)/p_0$ along the jet axis $y = 0$ (the circles are the experimental data, and the solid and dashed lines are the data calculated with and without taking the friction force into account).

From figures 3 and 4, it is evident that in both cases a supersonic underexpanded jet was ejected from the channel. If the friction force was absent, then the jet had a characteristic barrel shape. The presence of the friction force acting on the flow from the side of the nozzle walls led to the opening and formation of a fan jet. In a narrow jet (see figure 3), at the exit from the channel, a rarefaction wave propagated from the corner point inside the jet. In this rarefaction wave, the jet underwent acceleration to a supersonic speed. The action of the friction force on the jet from the side of the nozzle walls led to deceleration of the jet flow and to the formation of a weak closing shock wave in the section $x = 32\,\mathrm{mm}$ (see Fig. 3 (a, c)). Without taking into account the friction force, the Mach number in the jet was $\mathrm{M} = 2.4$, and with taking this force into account, we had $\mathrm{M} = 1.7$. In a wide jet (see Fig. 4), its acceleration proceeds in two rarefaction waves. The first rarefaction wave arises when the gas enters the wide channel with the formation of a separation region. The rarefaction wave is closed by a curvilinear shock wave, which on the axis has a coordinate $x = 15\,\mathrm{mm}$. The second rarefaction wave is formed when the gas flow leaves the channel moving into the slot. As a result of the action due to the friction force, the ejected jet becomes fan-shaped. Without taking the friction force into account, the maximum Mach number in the jet was $\mathrm{M} = 2.1$, and with taking this force into account the maximum Mach number was $\mathrm{M} = 1.7$. The calculated distributions of pressure along the jet axis proved to be in satisfactory agreement with the experimental results (see figures 3 (c) and 4 (c)).

Figure 5. The soot-oil film formed on the surface of the external disk during the outflow of the gas into the slot of height $h = 0.2$ mm in between the disks. The gas pressure in the pre-chamber is $p_0 = 0.9$ MPa .

The presence of a fan-shaped jet is also confirmed by the photo of the soot-oil film formed on the surface of the external disk (see figure 5).

5. Conclusion

The paper presents the results of numerical simulation and experiments in which supersonic jets in radial nozzles were studied. The radial nozzles differ from the conventional Laval nozzles by the involvement of a large surface area decelerating the gas flow. For narrow radial nozzles 0.2 mm wide, it was shown that the friction force acting on the flow from the side of the nozzle has a considerable influence on the flow structure. First, considerable deceleration of the jet occurs, and second, the jet acquires a fan-like shape. The results of numerical calculations were found to be in satisfactory agreement with experimental data.

Acknowledgments

This work was supported in part by the Russian Foundation for Basic Research (Grant No. 19-01-00292-a) and by the Government of the Russian Federation (Program for Basic Scientific Research of the State Academies of Sciences for the years 2013-2020 (Project AAAA-A17-117030610124-0)).

References

[1] Moller P 1966 *J. Basic Eng. Ser. D* **88** 153–4
[2] Kim S I and Park S O 2005 *Shock Waves* **4** 259–72
[3] Kiselev S P, Kiselev V P, Klinkov S V, Kosarev V F and Zaikovskii V N 2017 *Surf. Coat. Tech.* **313** 24–30
[4] Kiselev S P, Kiselev V P and Zaikovskii V N 2018 *Shock Waves* **28** 829–49
[5] Kiselev S P, Kiselev V Yu, Liapidevskii V P and Zaikovskii V N 2017 *J. Phys.: Conf. Ser.* **894** 012042
[6] Anderson D A, Tannehill J C and Pletcher R H 1984 *Computational Fluid Mechanics and Heat Transfer* (Hemisphere Publishing Corporation)